Antonio Soria-Verdugo*, Marco Tomasi Morgano, Hartmut Mätzing, Elke Goos, Hans Leibold, Daniela Merz, Uwe Riedel, Dieter Stapf,

Comparison of wood pyrolysis kinetic data derived from thermogravimetric experiments by model-fitting and model-free methods,

Energy Conversion and Management 212 (2020) 112818

The original publication is available at www.elsevier.com

https://doi.org/10.1016/j.enconman.2020.112818

Comparison of wood pyrolysis kinetic data derived from thermogravimetric experiments by model-fitting and model-free methods

Antonio Soria-Verdugo[a]*, Marco Tomasi Morgano[b], Hartmut Mätzing[c], Elke Goos[d], Hans Leibold[c], Daniela Merz[c], Uwe Riedel[d], Dieter Stapf[c]

[a] *Carlos III University of Madrid (Spain), Energy Systems Engineering Group, Thermal and Fluids Engineering Department. Avda. de la Universidad 30, 28911 Leganés, Madrid (Spain).*

[b] *ARCUS Greencycling Technologies GmbH, Leonberger Straße 30, D-71638 Ludwigsburg (Germany).*

[c] *Karlsruhe Institute of Technology (KIT), Institute for Technical Chemistry (ITC), Hermann-von-Helmholtz-Platz 1, 76344 Eggenstein-Leopoldshafen (Germany).*

[d] *Deutsches Zentrum für Luft- und Raumfahrt e.V. (German Aerospace Center, DLR), Institute of Combustion Technology, Pfaffenwaldring 38-40, 70569 Stuttgart (Germany).*

** corresponding author: asoria@ing.uc3m.es Tel: +34916248465.*

Abstract

The pyrolysis kinetics of beech wood was analyzed using model-free and model-fitting methods. Experimental measurements of the pyrolysis process were conducted in two thermogravimetric analyzers (TGA), a TG 209/2/F from Netzsch and a TGA Q500 from TA Instruments, which were found to have a similar precision in the establishment of the preset heating rate. Two experimental procedures were employed: (i) introducing samples which were pre-dried externally before the experiments were executed and (ii) internal (in

situ) drying of the samples in the TGA via a special temperature program below 150 °C which preceded the pyrolysis process.

The kinetic parameters were derived (i) using several model-free methods, namely Kissinger method, isoconversional methods, a simplified Distributed Activation Energy Model (sDAEM) and, (ii) using a model-fitting method via a five-step reaction model which calculates the differential thermogravimetric (DTG) curves at different heating rates; the calculated DTG curves were further analyzed by Kissinger's method to obtain overall kinetic data.

The kinetic parameters were found to be different in the two experimental procedures. Also, they turned out different when the assumed end temperature of the pyrolysis process was varied. This is because the pyrolysis of slowly charring solid residues becomes more important with increasing temperature and finally overruns the release of volatiles from the wood samples. For the same experimental procedure and for sufficiently low end temperatures, corresponding to a degree of conversion less than 85 %, model-free and model-fitting methods resulted in similar kinetic parameters.

Keywords**:** biomass pyrolysis; pyrolysis kinetics; model-free methods; model-fitting methods.

Nomenclature

A pre-exponential factor of rate coefficient [s^{-1}]

α degree of conversion [%]

β heating rate [K min^{-1}, K s^{-1}]

β_{mea} heating rate measured by the TGA [K min^{-1}, K s^{-1}]

β_{set} heating rate programmed to the TGA [K min^{-1}, K s^{-1}]

E activation energy [kJ mol^{-1}]

E_0 mean value of Gaussian distribution of activation energy [kJ mol^{-1}]

E_α activation energy for a specific value of the conversion degree [kJ mol^{-1}]

ε average relative error [%]

ε_A average relative error of the pre-exponential factor A [%]

ε_E average relative error of the activation energy E [%]

$f(\alpha)$ differential form of the α-dependent part of the rate equation [-]

$g(\alpha)$ integral form of the α-dependent part of the rate equation [-]

$h(E)$ probability density function of the activation energy [mol kJ^{-1}]

k rate coefficient/constant of a first-order reaction [s^{-1}]

m mass of the sample remaining [g]

m_0 initial mass of the sample at the beginning of TGA test [g]

m_{pi} mass of the sample remaining at the beginning of the pyrolysis [g]

m_{pf} mass of the sample remaining once the pyrolysis is completed [g]

n order of the pyrolysis reaction [-]

N total number of heating rates considered [-]

$\nu_{i,j}$ stoichiometric coefficient of carbon from component *i* in reaction *j* [-]

R universal gas constant [J mol^{-1} K^{-1}]

R^2 determination coefficient [-]

t time [min]

T temperature [ºC, K]

T_0 initial temperature of the pyrolysis process [ºC, K]

T_{max} temperature at which the reaction rate has its maximum [ºC, K]

X percentage of mass of the sample remaining [%]

X_{pi} percentage of mass remaining at the beginning of pyrolysis process [%]

X_{pf} percentage of mass remaining at the end of pyrolysis process [%]

Abbreviations:

CFD	Computational Fluid Dynamics
DTG	Differential Thermogravimetric
HHV	Higher Heating Value
KAS	Kissinger-Akahira-Sunose
LHV	Lower Heating Value
OFW	Ozawa-Flynn-Wall
sDAEM	simplified Distributed Activation Energy Model
TG	Thermogravimetric
TGA	Thermogravimetric Analysis / Thermogravimetric Analyzer

1. Introduction

Biomass is one of the most widely used renewable energy carriers due to its worldwide availability, its net carbon dioxide neutral character, and because it is easy to store, which permits decentralized production of heat and power on-demand. Furthermore, the local availability of biomass can increase fuel security and reduce carbon dioxide emissions associated with fuel transportation [1]. Biomass can be transformed via biochemical, physico-chemical, and thermochemical processes [2]. This paper is on pyrolysis, defined as thermal degradation in the absence of oxygen and other gasifying media [3]. Pyrolysis presents several benefits, such as the use of moderate temperatures (300-600 ºC), the mostly small amount of pollutant emissions, and the

possibility to obtain a high-quality liquid fuel, easy to handle, store and transport.

Pyrolysis of biomass can be studied using thermogravimetric analysis (TGA) or differential scanning calorimetry (DSC) [4]. The goal of TGA is to determine the global kinetic parameters of biomass pyrolysis processes (activation energies and pre-exponential factors), which in combination with other analytical measurement techniques helps to clarify the thermal decomposition process and to understand the product formation from the pyrolysis reactions. Moreover, these global kinetic data can also be employed for the design and optimization of pyrolysis reactors and as input parameters for CFD simulations [5].

The derivation of the kinetic parameters can be based on model-fitting or on model-free methods. Model-fitting methods require an assumption about the reaction mechanism and a suitable fit of the rate constants to match the overall results obtained from TGA measurements. In contrast, model-free methods assign only overall kinetic parameters to the decomposition process of the bulk sample. No effort is made in this case to clarify the product formation. Therefore, the computational procedure is relatively simple and the cost of model-free methods is low compared to the cost of model-fitting methods [6]. Vyazovkin et al. [7] consider that the kinetic parameters obtained from model-free methods are more consistent and reliable due to the absence of multiple assumptions made in model-based analyses. However, model-free methods yield less detailed information than model-fitting methods.

In previous studies of model-free methods, the fitting precision and the reliability of kinetic parameters were found to be directly related to the experimental

uncertainty, which can be high [8,9]. In contrast, high fitting precision was demonstrated to be realized using model-free methods [10]. This emphasizes the need for a critical comparison of the results obtained from model-free and model-fitting kinetic methods, which is the major objective of the present study.

In this work, the pyrolysis of beech wood was studied experimentally by non-isothermal thermogravimetric measurements performed in two different TGA instruments. The main novelty of the work relies on analyzing the experimental measurements conducted by two different research groups using two different TGA apparatus, by means of several model-free and a model-fitting method. Regarding model-free methods, various isoconversional models as well as the simplified Distributed Activation Energy Model (sDAEM), which is a multi-step method, were employed. In addition, a model-fitting method based on a five-step mechanism was used. Another innovation of this work is the use of different drying procedures for the beech wood samples. The different drying procedures tested were found to yield different pyrolysis kinetic data. Furthermore, the kinetic parameters were determined selecting different final temperatures for the pyrolysis process. In this way, the effect of the increasing contribution of secondary char pyrolysis to the whole pyrolysis process could be quantified.

2. Theory

Model-free methods permit the computation of the kinetic parameters for specific values of the pyrolysis conversion degree, requiring no assumptions about the reaction mechanism. Most of them describe biomass pyrolysis kinetics by an assumed single-step overall rate equation:

$$\frac{d\alpha}{dt} = k(T) f(\alpha), \tag{1}$$

employing the degree of conversion α, which is a dimensionless quantity, rather than the measured sample mass *m*. The rate of reaction dα/d*t* is expressed as a function of temperature *k(T)* and a function of the conversion *f*(α), which depends on the reaction order.

For consistency, the International System of units (kg, m, s, K) is used for all the variables included in the equations presented in this work.

For the rate coefficient, the most widely used temperature dependence expression is that proposed by Arrhenius [11]:

$$k(T) = A \exp\left(-\frac{E}{RT}\right), \tag{2}$$

where *A* is the pre-exponential factor, *E* is the activation energy, *R* is the universal gas constant, and *T* is the temperature. The resulting kinetic parameters may be dependent on the degree of conversion. Also, they may be understood to represent some average of all microscopic processes which contribute to the total pyrolysis process. Model-free methods include Kissinger's method, isoconversional methods, and multi-step methods, like the simplified Distributed Activation Energy Model (sDAEM), which are described in detail below. The Kinetics Committee of the International Confederation for Thermal Analysis and Calorimetry (ICTAC) recommends the calculation of kinetic parameters from isoconversional models for a wide range of conversion values, from 5% to 95% [7]. In addition, the sDAEM has been widely used to derive pyrolysis kinetic data.

Model-fitting methods interpret and approximate the measured mass loss (i) by generalized reaction mechanisms, templates of which are available in the literature [12-14] or (ii) by individually developed reaction mechanisms, which usually involve a set of several first order reactions.

The template reaction mechanisms (i) represent decomposition processes which are relevant to any type of solids, not only solids of biogenic origin. Hence, they focus on n-th order reaction mechanisms, on the evolution of lattice defects in crystals, on diffusion limited decompositions, etc. In contrast, individually developed reaction mechanisms (ii) involve explicit reaction schemes which were developed for the specific substance under investigation, like the famous Broido-Shafizadeh models for the pyrolysis of cellulose [15,16] and numerous modifications and refinements thereof, as reviewed by Antal et al. [17] and by Conesa et al. [18]. Of course, the published reaction mechanisms vary considerably in the detailed description of various decomposition pathways, some of them [19] even consider thermodynamic data of the involved substances and specific processes at the molecular level, as reviewed recently by Wang et al. [6]. In practice, a good compromise is sought between user friendly applicability, completeness and accuracy.

It is emphasized here that the rate constants of such explicit mechanisms are not generally valid, because they do not refer to elementary reactions, but to composite reactions of biopolymers. Therefore, none of the reported rate constants is applicable to a different reaction scheme. They are valid only within the frame of the particular reaction mechanism for which they were developed. Other limitations of global mechanisms are the neglect of reverse reaction

pathways and of heat release or consumption, but this is beyond the scope of this paper.

As noticed repeatedly in the literature, the kinetic data (*A*, *E*) derived from model-fitting or from model-free approaches vary substantially; famous examples are the round robin studies of the thermal decomposition of cellulose [20] and calcium carbonate [21]. Besides systematic errors, the data handling and the methods of data evaluation came into focus and were shown to contribute to the scattering of kinetic results [21-23].

2.1. Kissinger method

The Kissinger method [24,25] is based on the differential form of the rate equation. It relates the temperature T_{max}, at which the rate of reaction, $d\alpha/dt$, reaches a maximum, to the heating rate β. In case of a first order reaction, the relation reads:

$$\ln\left(\frac{\beta}{T_{\max}^2}\right) = \ln\left(\frac{AR}{E}\right) - \frac{E}{RT_{\max}}. \qquad (3)$$

This characteristic equation can be employed to determine the pre-exponential factor *A* and the activation energy *E* of the pyrolysis reactions from a set of differential thermogravimetric (DTG) curves obtained at different heating rates β. Eq. (3) is exact only for single and pure substances which decompose according to a first-order reaction. However, for complex solid fuels such as biomass, Kissinger's method produces single values of *A* and *E* averaged over all individual physico-chemical processes, which in reality vary with the degree of conversion α. Therefore, the results obtained from the Kissinger method should be considered carefully. It is recommended to cross-check the

dependence or independence of the kinetic parameters on the degree of conversion by an isoconversional method or by sDAEM [26].

2.2. Isoconversional methods

The isoconversional methods can be classified into differential and integral methods, depending on the form of the rate equation on which they are based [6]. The only differential isoconversional method of practical importance is the Friedman method [27], whereas a variety of integral isoconversional methods are in common use, e.g., the Ozawa-Flynn-Wall (OFW) method [28,29] and the Kissinger-Akahira-Sunose (KAS) method [24,30].

The characteristic equation of the Friedman model, Eq. (4), is obtained directly from the logarithm to the differential form of the rate equation, Eq. (1). For the assumed first order kinetics of the pyrolysis process, $f(\alpha) = 1 - \alpha$ [31], hence:

$$\ln\left(\frac{d\alpha}{dt}\right) = \ln\left(A(1-\alpha)\right) - \frac{E}{RT}. \tag{4}$$

The integral isoconversional methods make use of the integral form of the rate equation:

$$g(\alpha) = \int_0^{\alpha} \frac{d\alpha}{f(\alpha)} = \frac{A}{\beta}\int_{T_0}^{T} \exp\left(-\frac{E}{RT}\right)dT \approx \frac{A}{\beta}\int_0^{T} \exp\left(-\frac{E}{RT}\right)dT. \tag{5}$$

This integral employs the isoconversional principle according to which A and E are independent of temperature. The lower integration limit T_0 can be approximated by 0, since usually the degree of conversion below the starting temperature is negligible [28]. The integral in Eq. (5) is the so-called

temperature integral, *I(E,T)*. It has no analytical solution, thus, Eq. (5) needs to be solved by approximation or by numerical integration [26].

The OFW [28,29] method uses the approximation of Doyle in Eq. (5) [32]. For first order reactions, the function *g* is $g(\alpha) = -\ln(1-\alpha)$ [31], and the OFW characteristic equation yields:

$$\ln\beta = \ln\left(-\frac{AE}{R\ \ln(1-\alpha)}\right) - 5.3305 - 1.052\frac{E}{RT}. \tag{6}$$

The Kissinger-Akahira-Sunose (KAS) method [24,30] improves the accuracy of the OFW method by using the approximation of Murray and White [33] for the temperature integral instead of Doyle's approximation. The characteristic equation then reads:

$$\ln\left(\frac{\beta}{T^2}\right) = \ln\left(-\frac{AR}{E\ \ln(1-\alpha)}\right) - \frac{E}{RT}. \tag{7}$$

Further details of the mathematical derivation of the isoconversional kinetic methods can be found elsewhere [10, 34]. Corresponding to the validity of the approximations to the temperature integrals, the expected numerical accuracy of KAS method is higher than that of OFW method.

2.3. Simplified Distributed Activation Energy Model (sDAEM)

The Distributed Activation Energy Model (DAEM) proposed by Vand [35] assumes the pyrolysis of a solid fuel to be a superposition of a large number of independent first-order Arrhenius type reactions with different activation energies, which can be represented by a continuous probability density function

h(E), with units of inverse activation energy. For a constant heating rate β = d*T*/d*t*, the degree of conversion α for the original DAEM can be written:

$$\alpha = 1 - \int_0^\infty \exp\left[-\frac{A}{\beta} \int_0^T \mathrm{e}^{-E/RT} \mathrm{d}T \right] h(E)\, \mathrm{d}E. \tag{8}$$

The exponential function in Eq. (8) is the so-called ϕ function. For the original DAEM, the form of the probability density function of the activation energy should be assumed to follow any statistical distribution like Gaussian, Weibull, etc. Thus, the original DAEM is an implicit model-fitting kinetic method.

Miura [36] and Miura and Maki [37] proposed a simplified DAEM (sDAEM), which is an integral model-free multi-step method. In view of the rapid variation of the ϕ function from 0 to 1, Miura [36] proposed to approximate it by a step function for any specific value of the activation energy. Using the approximation of Coats and Redfern [38] for the temperature integral and the approximate value of 0.58 for the step variation, the ϕ function becomes:

$$\phi(E,T) = \exp\left[-\frac{A}{\beta} \int_0^T \mathrm{e}^{-E/RT} \mathrm{d}T \right] \approx \exp\left[-\frac{ART^2}{\beta E} \mathrm{e}^{-E/RT} \right] = 0.58. \tag{9}$$

Then, taking logarithms to Eq. (9), the characteristic equation for the sDAEM is:

$$\ln\left(\frac{\beta}{T^2} \right) = \ln\left(\frac{AR}{E} \right) + 0.6075 - \frac{E}{RT}. \tag{10}$$

Therein, *A* and *E* usually vary with α. Miura and Maki [37] proposed the use of several TG curves, measured at several constant heating rates β, to determine *A* and *E* for each value of α. Soria-Verdugo et al. [39,40] found that at least five TG curves should be used in order to reproduce the measured TG curves with

reasonable accuracy. Moreover, characteristic sDAEM equations for time dependent heating rates are available now [40,41]. Overall, the numerical accuracy of the sDAEM method is estimated to be comparable to the KAS method.

2.4. Model-fitting kinetic method

Originally, a three-step mechanism was developed for the independent decomposition of the three pseudocomponents, i.e., hemicellulose, cellulose, and lignin. Despite its plausibility, such an approach has limitations, because no particular consideration of the polymeric nature of the biomass is made, effects of inorganic constituents are neglected, etc. [43]. Moreover, such a model predicts the separation of the hemicellulose and cellulose peaks at low heating rates [44,45], which is contrary to experimental evidence [46]. This can be avoided by increasing the number of reactions. The five-step model includes two parallel decomposition pathways for cellulose, one of which leads to intermediate tar formation. As default tar species levoglucosan was chosen, because it is a key species of wood pyrolysis and since the overall tar composition can be approximated by $C_6H_{10}O_5$, which is the sum formula of both the cellulose monomer and levoglucosan [46-49]. The five-step model is listed in Table 1.

Table 1: Reaction scheme of the five-step model [45,50].

compound	**reaction**[1)]	**A** $[s^{-1}]$	**E** [kJ/mol]
cellulose	$C_6H_{10}O_5 \rightarrow$ gas + 2.5 C	$2 \cdot 10^8$	132
cellulose	$C_6H_{10}O_5 \rightarrow$ 0.75 tar + gas + 0.625 C	$3 \cdot 10^{13}$	195
hemicellulose	$C_5H_8O_4 \rightarrow$ gas + 2 C	$1 \cdot 10^7$	105
lignin	$C_{10}H_{10}O_4 \rightarrow$ gas + 4.3 C	$1.5 \cdot 10^{14}$	192
tar	$C_6H_{10}O_5 \rightarrow$ gas	$2 \cdot 10^7$	122

[1)] gas composition is not a subject in this work; therefore, it is not specified here

The pseudocomponents are represented by their monomeric formulas and "gas" is a mixture of carbon monoxide (CO), carbon dioxide (CO_2), methane (CH_4), hydrogen (H_2) and water vapor (H_2O) to complete the stoichiometry. Within this model, methane is a lump species which stands for all the non-tar hydrocarbons [50]. The kinetic data were obtained by manual fits to experimental DTG curves of several beech wood samples. The quality of such data fits is usually assessed by comparison to a model-free approach. Recently, the five-step model was extended to include dual decomposition reactions for all pseudo-components and two different tar species [51].

The kinetic parameters derived from these kinetic methods, either model-free or model-fitting, could be used in combination to heat and mass transfer models to simulate the pyrolysis process of wood in a bench scale or even industrial unit. The validity of the kinetic results derived from these methods for a bench scale facility was already demonstrated by Tomasi Morgano [52], however, the validity for industrial units should be evaluated.

3. Materials and methods

3.1. Feedstock analysis

European beech wood, *Fagus sylvatica*, was adopted for this study. Bark-free grinded material, particle size of 0.5-1.0 mm, was purchased from J. Rettenmaier und Söhne GmbH & Co. in Rosenberg, Germany. The feedstock was selected due to the extensive data available in the literature as well as for its high reproducibility and constant chemical composition.

Analysis of the feedstock was carried out following the respective German DIN Standards [53]. The chemical composition was determined by the Klason and Kürschner standards [54] to evaluate the content of cellulose, hemicellulose and lignin. The results of the analysis are reported in Table 2. Considering the characteristics of beech wood reported in Table 2, the results of the kinetics analysis performed in this work are specific for wood. The results may differ for different solid samples such as polymers, coal, or non-lignocellulosic biomass.

Table 2: Characterization of the feedstock European beech wood (*Fagus sylvatica)*.

Parameter	Method	Value	Unit
Moisture	DIN EN 14774-2	9.7	wt.% ar
Proximate analysis			
Ash (550°C)	DIN EN 14775	1.4	wt.% db
Volatile matter	DIN EN 15148	83.3	wt.% db
Fixed carbon	analog to DIN 51734	15.3	wt.% db
Elemental analysis			
Carbon	DIN EN 15104	49.5	wt.% db
Hydrogen	DIN EN 15104	6.0	wt.% db
Nitrogen	DIN EN 15104	0.19	wt.% db
Oxygen*	DIN EN 15296	42.9	wt.% db
Trace elements			
Sulfur	DIN EN 15289	0.016	wt.% db
Chlorine	DIN EN 15289	< 0.005	wt.% db
Fluorine	analog to DIN EN 15289	< 0.001	wt.% db
Calorific values			
HHV	DIN EN 14918	19530	kJ/kg db
LHV	DIN EN 14918	18230	kJ/kg db
Chemical analysis			
Cellulose	Kürschner	44.9	wt.% daf
Hemicellulose	Sodium Chlorite $NaClO_2$[#]	33.9	wt.% daf
Lignin	Klason	21.2	wt.% daf

ar is as received; db is dry basis; daf is dry ash-free basis

* calculated by difference

[#] calculated from holocelullose

3.2. Thermogravimetric analyzers

Two different thermogravimetric analyzers (TGA) were employed to conduct pyrolysis tests: a TGA Q500 from TA Instruments located at BIOLAB in University Carlos III of Madrid (UC3M), Spain and a TG 209/2/F from Netzsch located at the Institute for Technical Chemistry in Karlsruhe Institute of Technology (KIT), Germany. The technical specifications of both TGA instruments are included in Table 3, where the similarity of both devices can be seen.

Table 3: Technical specifications of TGA Q500 and TG 209/2/F.

Parameter	**TGA Q500**	**TG 209/2/F**
Maximum sample mass [g]	1	1
Mass measurement precision [%]	± 0.01	± 0.01
Mass resolution [μg]	0.1	0.1
Pan volume [μl]	100	85
Pan material	Platinum	Aluminum oxide
Furnace nitrogen flow rate [ml/min]	60	15
Balance nitrogen flow rate [ml/min]	40	10
Heating rate range [ºC/min]	0.01 – 100	0.1 – 80

The monitored variables during the pyrolysis tests in both TGA apparatus, i.e., time t, temperature T, percentage of mass remaining X, and variation of the percentage of mass remaining dX/dt, were recorded in temperature intervals of 0.1 ºC.

3.3. Pyrolysis measurements in TGA

The recommendations of the ICTAC kinetics committee [55] were considered for collecting the experimental thermal analysis data used for the kinetic computations. The initial sample mass was 10.5±0.5 mg. This mass is low enough to guarantee a negligible effect of heat and mass transfer inside the sample, while providing a high signal-to-noise ratio during the measurements.

The pyrolysis process was studied in two different procedures:

(i) external drying (experiments with pre-dried samples)

In these experiments, the wood samples were dried in a heated oven at 105 °C for 24 hours to obtain a residual moisture close to 5 % and were protected against ambient atmosphere until usage. During pyrolysis, the temperature was increased from room temperature to 900 ºC at constant heating rates of 5, 10, 15, 25, 35, and 50 ºC/min. All experiments were repeated twice both in the TGA Q500 and in the TG 209/2/F. The heating rates are low in comparison to industrial applications; however, the kinetic parameters were previously found to be independent of the heating rate in the range 20 – 200 ºC/min for some biomass samples [56,57].

(ii) internal drying (in situ drying of the samples)

In these experiments, the samples were introduced into the TGA as received, i.e., containing approximately 10 wt.% of humidity, and a two-stage heating pyrolysis was used in the TGA tests [58]. The temperature was first increased to 105 °C and kept at that level for roughly 30 min, before starting the pyrolysis and heating up further to 900 °C. The same six different values of the heating rate as for the external drying tests were used for the in situ drying tests. The pyrolysis of the in situ drying samples was conducted only in the TGA Q500 to quantify the effect of the in situ process by comparison with the results of the pre-dried samples.

3.4. Processing of the TGA data

As already mentioned, the five-step model [45] was developed by manually fitting the experimental DTG results of several beech wood pyrolysis experiments to the set of five first order reactions, Table 1. For this purpose, the initial composition of beech wood was set to 45 wt.% cellulose, 34 wt.% hemicellulose and 21 wt.% lignin (daf, see Table 2). The total initial mass, the starting temperature T_0 and the heating rate β were set to the experimental conditions. The time derivative of the mass of each pseudocomponent *i* in reaction *j* was set to:

$$\frac{\mathrm{d}m_{i,j}}{\mathrm{d}t} = -A_{i,j} m_{i,j} \exp\left(-\frac{E_j}{RT}\right), \tag{11}$$

where the evolution of temperature T with time t is linear $T = T_0 + \beta \cdot t$. Note that, of course, since cellulose has two decomposition pathways in the five-step model, the time derivative of its mass is the sum of two rate expressions (j = 1 and 2). Similarly, the time derivative of carbon (char) formation is:

$$\frac{\mathrm{d}m_C}{\mathrm{d}t} = \sum_j \sum_i A_{i,j} \nu_{i,j} m_{i,j} \exp\left(-\frac{E_j}{RT}\right), \tag{12}$$

where $\nu_{i,j}$ is the stoichiometric coefficient of carbon from component *i* in reaction *j*. The differential equations were solved to obtain, amongst others, the total solid mass (TG curve) and its time derivative (DTG curve) as a function of time and temperature using a double precision version of the LSODE package from Lawrence Livermore National Laboratory (LLNL) [59]. The numerical values for $\nu_{i,j}$, $A_{j,j}$ and E_j are listed in Table 1 in section 2.4.

All model-free methods are based on the degree of conversion α and its rate of variation dα/dt which were determined from the monitored variables of both TGA apparatus. The degree of conversion α varies between 0 % at the beginning of the pyrolysis process and 100 % when the pyrolysis is completed. The degree of conversion α can be calculated as:

$$\alpha = 100 \cdot \frac{m_{pi} - m}{m_{pi} - m_{pf}}, \tag{13}$$

where m is the mass of the sample remaining at time t and m_{pi} is the initial mass of the sample when pyrolysis starts, i.e., at 150 ºC, and m_{pf} is the final mass of the sample once the reaction is completed. Its value varies a little depending on the temperature which is chosen to be the final temperature of the pyrolysis process. Then, dividing by the initial mass of the sample employed in the TGA test m_0, the degree of conversion α can be expressed in terms of the current mass percentage which is the output reading of the instruments:

$$\alpha = 100 \cdot \frac{X_{pi} - X}{X_{pi} - X_{pf}}. \tag{14}$$

In view of the definition of the degree of conversion α as a function of the percentage of mass remaining X, Eq. (14), the rate of variation of α can be related to the rate of variation of X as:

$$\frac{\mathrm{d}\alpha}{\mathrm{d}t} = -\frac{1}{X_{pi} - X_{pf}} \frac{\mathrm{d}X}{\mathrm{d}t}. \tag{15}$$

4. Results and discussion

4.1. Precision of heating rates in the two TGA instruments

In a TGA, the desired change of the sample temperature with time is pre-set by the programmed heating rate. However, the real sample temperature lags behind the programmed temperature and behind the temperature reading. The exact discrepancy is due to several instrument properties and operation conditions like location of the thermocouple, nature and flow rate of the inert carrier gas, heating rate, sample mass and particle size distribution, as well as the reaction heat. The thermal lag error increases at faster scanning rates, larger sample masses, higher weight sample pans, etc. Therefore, the capability of the TGA to maintain the heating rate at a constant value β_{set} during the whole process is a characteristic of the instrument with the pan system, the employed experimental conditions and the sample itself. To compare the instruments' performance considering their specifications and the given different operation conditions (Table 3 without considering the maximum sample mass) the heating rates obtained in both TGAs during all the beech wood pyrolysis tests were determined in a post-processing procedure as the time derivative of the temperature output reading. This parameter is denoted β_{mea}. A moving average filter of 250 points was used for the calculation of β_{mea} to avoid the numerical noise produced by the derivation. The comparison of both TGA instruments in terms of their capability to maintain the heating rate at β_{set} was carried out based on the relative error of the heating rate:

$$\varepsilon_{\beta} = \frac{\beta_{set} - \beta_{mea}}{\beta_{set}}. \tag{16}$$

The values of ε_{β} are plotted in Figure 1 as a function of temperature for all the pyrolysis experiments conducted in both TGA instruments. In both cases, the

accuracy of the equipment to maintain a set value for the heating rate is higher for low heating rates and for high temperatures, as a consequence of the time required by the instruments to adjust to the programmed value of β. However, the behavior of both TGAs differs, especially for high values of the heating rate. The TGA Q500 approaches the selected value of β from slightly lower values, whereas the TG 209/2/F seems to overshoot the set value of β and approximate to it from higher values. This results in positive values for the relative error of the heating rate, Eq. (16), for the TGA Q500, whereas negative values of ε_β were obtained for the TG 209/2/F. In terms of the deviation from the selected value of the heating rate, the TGA Q500 is very accurate for the whole range of temperatures analyzed for values of β below 25 ºC/min. In contrast, deviations similar to those obtained in the TGA Q500 for heating rates of 35 ºC/min occur in the TG 209/2/F for values of 15 ºC/min. In addition, the maximum variations for heating rates up to 50 ºC/min in the temperature range of 150 – 600 ºC is 8.5 % for the TG 209/2/F and 4 % for the TGA Q500. Nevertheless, for temperatures above 300 ºC, where most of the pyrolysis of lignocellulosic biomass occurs, the deviations of the heating rate are within 1.5 % for the TGA Q500 and 5 % for the TG 209/2/F, which are acceptable values in both cases.

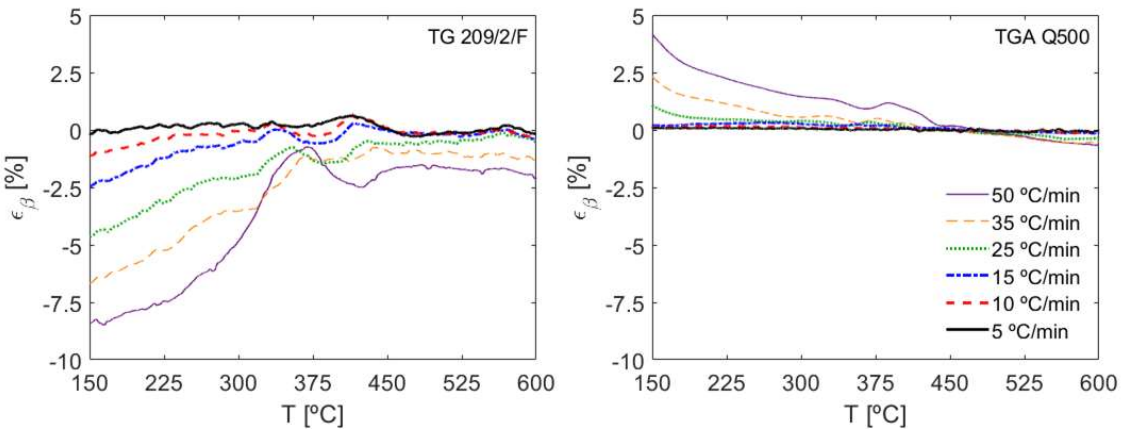

Figure 1: Relative error of the heating rate for all the pyrolysis tests in both TGA instruments during the pyrolysis of the pre-dried samples.

4.2. TG and DTG curves obtained for the pre-dried samples in both TGAs

The measured TG and DTG curves for the pre-dried beech wood samples are plotted in Figure 2 for both instruments.

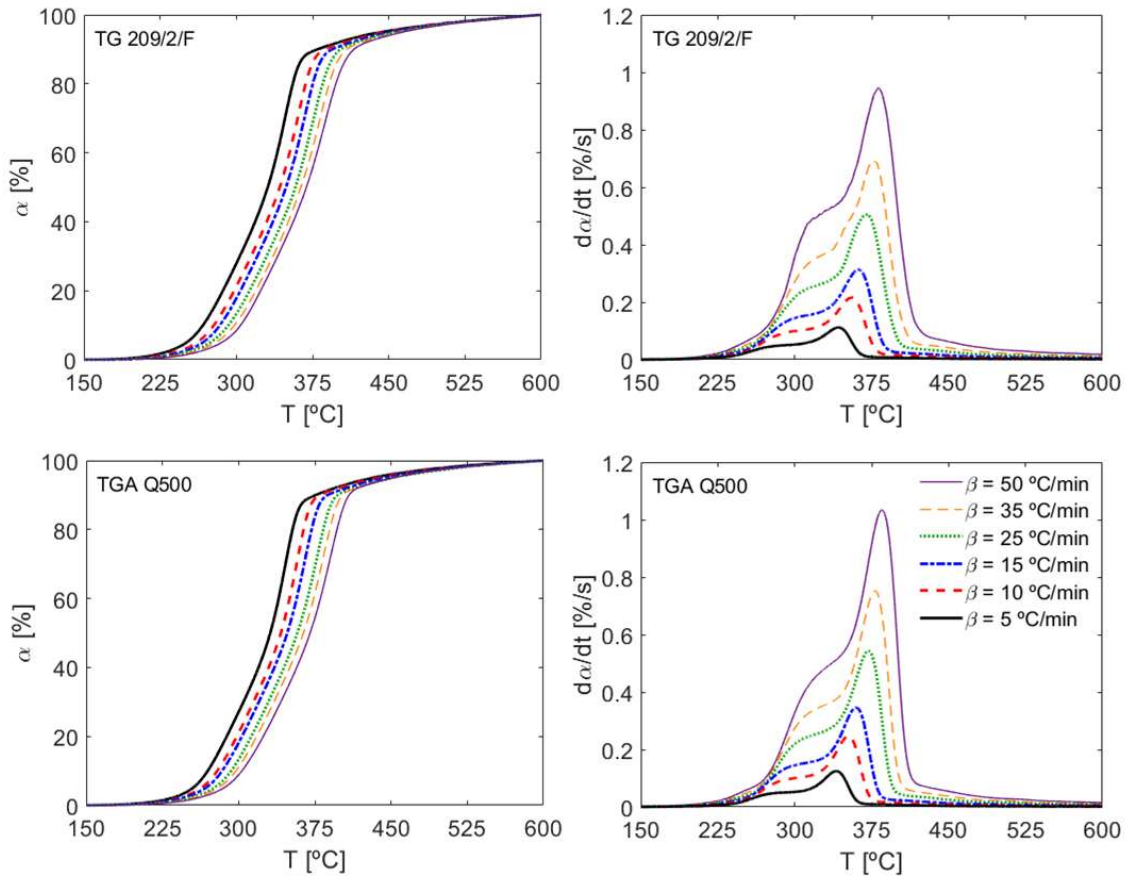

Figure 2: TG and DTG curves for the pyrolysis of beech wood at various heating rates in both TGA instruments (pre-dried samples).

The TG curves show a steep increase of the degree of conversion in a temperature range between approximately 250-400 ºC, followed by a smooth increase of the degree of conversion towards higher temperatures, for all the heating rates tested. In this temperature range, most of the volatile matter

contained in lignocellulosic biomass is released and decomposed, followed by the subsequent slow pyrolysis of the char produced. As a consequence of the non-isothermal experimental procedure, an increase of the heating rate β induces a shift of the decomposition process to higher temperatures, in agreement with literature data [25,60,61].

The structure of the DTG curves has often been interpreted to originate from overlapping peaks in the literature. In this sense, two overlapping peaks can be observed at temperatures between 250 and 400 ºC. These may be attributed to the pyrolysis of the hemicellulose and cellulose. A third underlying peak, which covers a wide range of temperatures between 200 ºC and 500 ºC, cannot be observed directly, but is expected to represent the comparatively slow pyrolysis of lignin [47].

For the pre-dried samples, the agreement between the experimental results obtained in the two thermogravimetric analyzer TG 209/2/F and TGA Q500 was good with relative errors around 2 % in α for TG and 10 % in dα/dt for DTG data. The differences are probably due to small differences of the thermal lags.

4.3. Results of model-free methods

4.3.1. Pre-dried samples

From the TG and DTG curves shown in Figure 2, characteristic plots were prepared for the model-free methods, i.e., Kissinger, Friedman, OFW, KAS, and sDAEM. In the Kissinger plot, the logarithm of the heating rate β over the temperature squared, T_{max}^2, for which the rate of reaction dα/dt is maximum (Figure 2) is plotted as function of the inverse of this temperature, $1/T_{max}$, Eq.

(3). Since the maximum rate of reaction is attained at a specific temperature for each heating rate, the Kissinger plot has only one data point for each heating rate.

According to the Friedman characteristic equation Eq. (4), the Friedman plot shows the values of the logarithm of the rate of reaction $\mathrm{d}\alpha/\mathrm{d}t$ versus the inverse temperature $1/T$. The OFW plot represents the logarithm of the heating rate β, left-hand-side of the OFW characteristic equation Eq. (6), as a function of the inverse temperature $1/T$. Finally, KAS and sDAEM are based on similar characteristic equations Eq. (7) and Eq. (10), respectively, hence their plots coincide, depicting the logarithm of the heating rate β over temperature squared versus the inversed of temperature $1/T$ in both cases. The four different plots obtained from the pyrolysis measurements of beech wood conducted in the TG 209/2/F for the pre-dried samples are included in Figure 3. The plots derived from the measurements performed in the TGA Q500 are very similar to those shown in Figure 3, therefore, they are not included in the figure to avoid repetition.

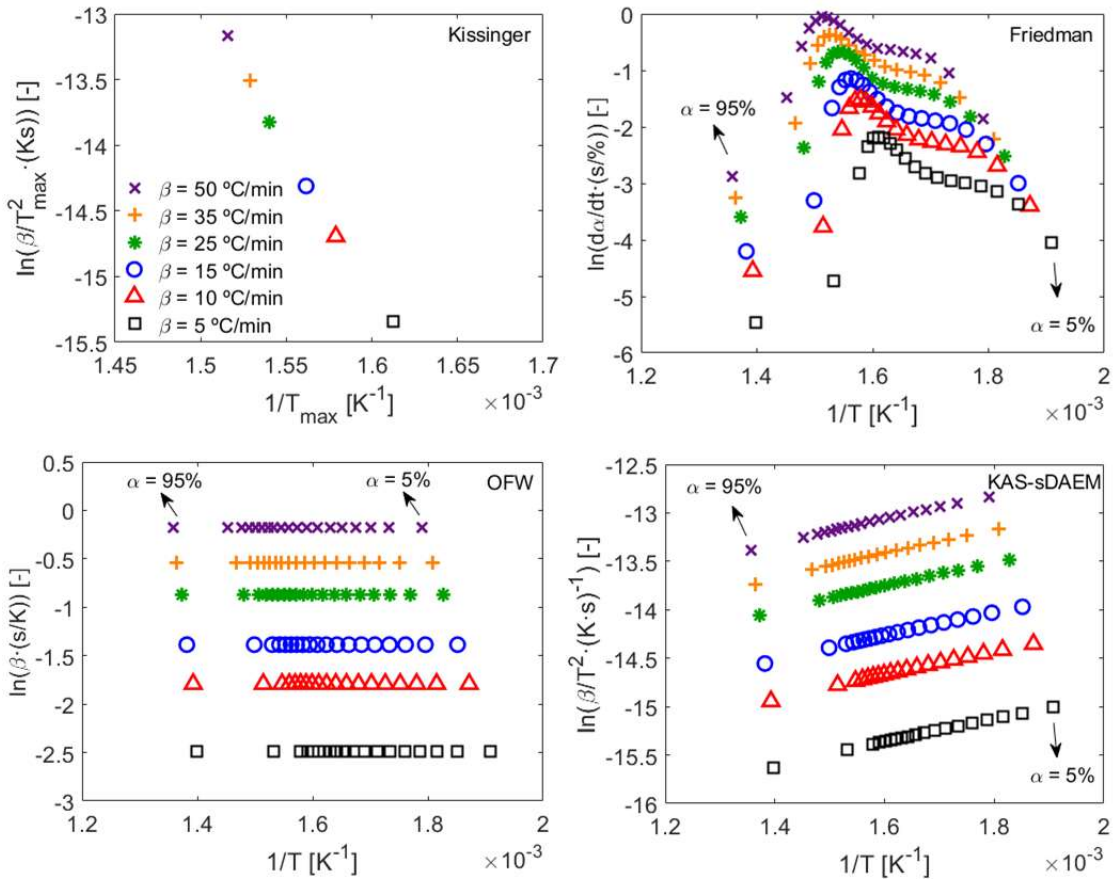

Figure 3: Data evaluation according to the different model-free kinetic methods applied to the pyrolysis measurements conducted in the TG 209/2/F (pre-dried samples).

The linearity of the data represented in the characteristic plots of Figure 3 is high, with coefficients of determination $R^2 \geq 0.995$ (Table 4), averaged in a degree of conversion range from 5% to 95%. The high R^2 values obtained from the pyrolysis measurements of pre-dried beech wood in both the TG 209/2/F and TGA Q500, reported in Table 4, reflect the high quality and reliability of the experimental measurements conducted in both instruments [9] and confirms the first-order assumption for the pyrolysis reactions.

Table 4: Coefficients of determination R^2 for the linear fitting of the characteristic plot data obtained from the pre-dried beech wood pyrolysis measurements in the TG 209/2/F and the TGA Q500.

	Kissinger	Friedman	OFW	KAS-DAEM
TG 209/2/F	0.998	0.997	0.999	0.995
TGA Q500	0.995	0.998	0.996	0.998

From the slope and intercept of the linear fits to the data in the characteristic plots, the pre-exponential factor *A* and activation energy *E* can be derived according to the characteristic equations. The values of the pre-exponential factors *A* and the activation energies *E* are shown in Figure 4 for a range of degree of conversion from 5 % to 95 %. The results from the two thermogravimetric analyzers are very similar. The conversion dependent values of *A* and *E* obtained from both the isoconversional methods and sDAEM show a similar behavior, with a roughly uniform value for a wide range of pyrolysis conversions from 5 % to around 85 %. Towards higher degrees of conversion, the values for *A* and *E* increase suddenly. This corresponds to the final slowdown of the conversion rate as seen in Figure 2. Hence, this is probably due to a dominance of the final char conversion processes.

As is obvious from Figure 4, the kinetic parameters obtained in the two instruments, by sDAEM and the isoconversional kinetic methods (KAS, OFW and Friedman) resulted in very similar values of *ln A* and *E*, differing by only 5-6 %. In contrast, Kissinger's method gave notably different values for *ln A* and *E* in the two instruments, differing by more than 20 %. Such deviations can be attributed to the simplicity of this data evaluation method and its differential character, which is liable to overrate the instrument noise, resulting in a

reduction of the accuracy of the data evaluation [31]. The results of the kinetic parameters of beech wood pyrolysis derived in this work, shown in Figure 4, are in good agreement with those reported previously by Branca et al. [44], Ding et al. [62], Grønli et al. [63], and Di Blasi and Branca [64].

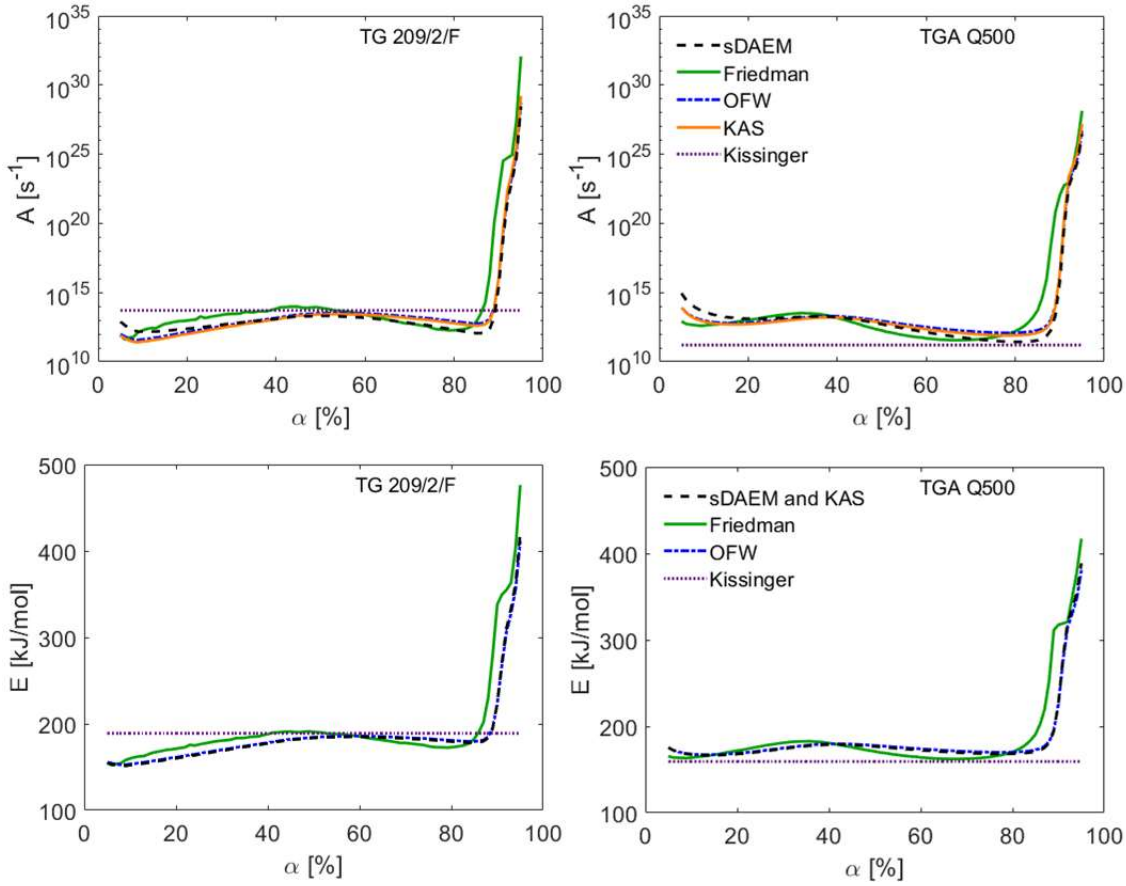

Figure 4: Kinetic parameters obtained from the various model-free kinetic methods applied to the pyrolysis measurements of pre-dried beech wood conducted in the TG 209/2/F and TGA Q500.

4.3.2. In situ dried samples

The results obtained from the pyrolysis of the in situ dried samples performed in the TGA Q500 were postprocessed similarly to the results of the pre-dried samples, using the same temperature range to determine the conversion degree, i.e., from 150 to 600 ºC, and applying the sDAEM to derive the kinetic

parameters of the pyrolysis. The variations of the pre-exponential factor *A* and the activation energy *E* with the pyrolysis conversion degree α are shown in Figure 5 for the in situ and pre-dried tests carried out in the TGA Q500. The values of the kinetic parameters for the pre-dried and in situ dried samples are similar, obtaining average deviations of 3.2 % for *ln A* and 5.3 % for *E* over a range of the conversion degree from 5% to 85 %. However, a higher difference is obtained for high values of the conversion degree, corresponding to the pyrolysis of char, for which the kinetic parameters obtained applying sDAEM to the in situ dried samples are lower than those derived from the pre-dried samples. In view of the effect of humidity on the kinetic parameters of pyrolysis, drying the samples prior to the TGA pyrolysis tests (pre-drying) is recommended. However, if the sample must be dried in the TGA (in situ drying), the drying and pyrolysis processes should be properly separated by using a two-stage heating for the TGA pyrolysis tests to prevent any effect of humidity of the pyrolysis reactions.

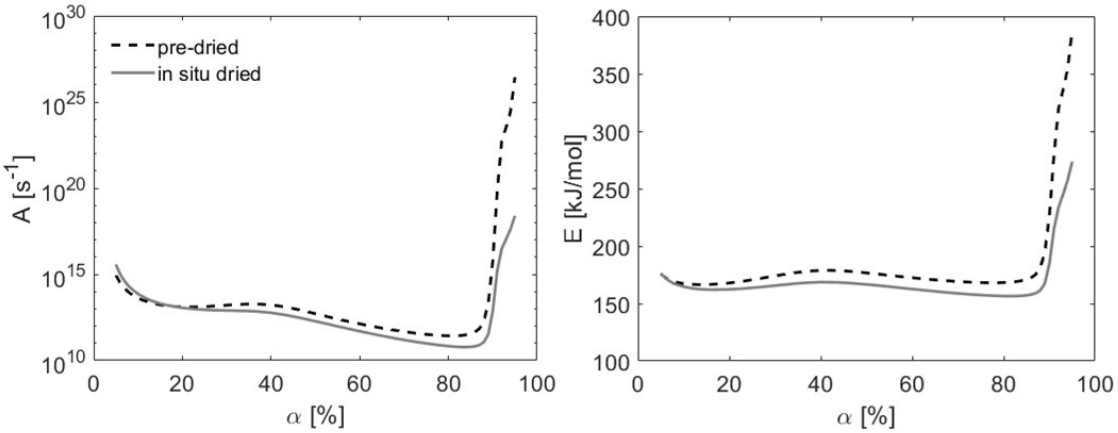

Figure 5: Kinetic parameters obtained applying sDAEM to the pyrolysis measurements of pre-dried and in situ dried beech wood samples in the TGA Q500.

4.4. Results of the five-step model

Figure 6 shows Kissinger plots of the experimental data for the pre-dried and the in situ dried samples and compares them to the Kissinger plot that results from the five-step model. For the pre-dried samples, the experimental data obtained from the TG 209/2/F and TGA Q500 are in good agreement. However, if in situ drying is applied, the temperatures of maximum decomposition rate, T_{max}, systematically decrease by around 15 K and the obtained kinetic parameters are in closer agreement with the five-step model results. Perhaps, pre-drying and in situ drying result in different surface properties and/or in different pore structures, which lead to some change in the pyrolysis rate and/or reactions.

The resulting kinetic parameters are tabulated in Table 5. While all activation energies are similar and are in the range E = 170 ± 15 kJ/mol for all cases, the ordinate intercepts are quite different. In fact, the pre-exponential factors differ by more than two orders of magnitude, giving $A = 10^{12.14\pm1.14}$ s^{-1}. Note, however, that such a comparison has limitations, because it is based on the simplification of Kissinger's method and because only one temperature is considered. A better unifying view is presented in section 4.6 below.

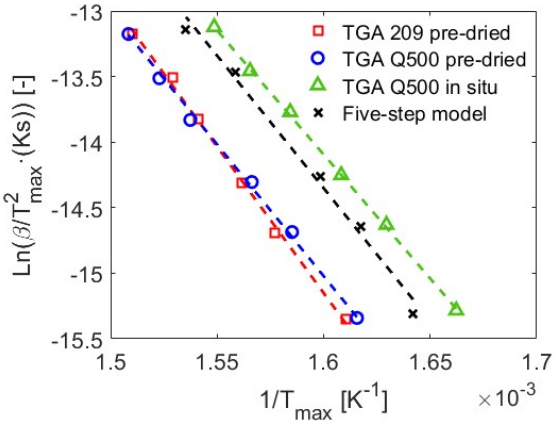

Figure 6: Kissinger plots of experimental data and five-step model.

Table 5: Comparison of overall kinetic data obtained from experiments and the five-step model (Kissinger's method applied to both experimental and calculated data).

Data set	A [s^{-1}]	E [kJ/mol]
TG 209/2/F, pre-dried	$1.9 \cdot 10^{13}$	185.4
TGA Q500, pre-dried	$5.3 \cdot 10^{11}$	166.9
TGA Q500, in situ dried	$2.0 \cdot 10^{11}$	157.2
Five-step model (TG 209/2/F)	$1.3 \cdot 10^{12}$	168.0

4.5. Effect of the final temperature selected for the pyrolysis process

The calculation of the degree of conversion by Eq. (14) is based on the selection of appropriate initial and final temperatures for the pyrolysis process. The selection of these temperatures may affect the results obtained for the kinetic parameters of the pyrolysis reaction, because (i) in the initial stage, up to about 120 °C, the mass loss is due to the drying process, (ii) in the final stage, above about 400 °C, the mass loss is mainly due to the thermal decomposition of the residual char.

Only in between these temperatures, the mass loss is really dominated by the release of original volatile matter. Therefore, the initial temperature should be selected as a value higher than the drying temperature, i.e., around 100 ºC for atmospheric processes, and below the minimum temperature for the onset of the release of volatiles. The value selected for the initial temperature has only little effect on the kinetic results provided that the degree of pyrolysis conversion below this value is negligible. A typical value is 150 ºC, since the devolatilization

of biomass occurs at temperatures above this value. In contrast, the proper choice of the end point of the pyrolysis process is not so easy to define *a priori*.

Figure 7 a) shows the evolution with temperature of the percentage of mass remaining in the TGA Q500, *X*, during the pyrolysis of beech wood at a heating rate of 5 ºC/min. The slope of the curve of mass percentage versus temperature is negligible for a temperature around 150 ºC, thus, this is a proper value for the initial temperature of the pyrolysis process. Furthermore, the selection of a different value for the initial temperature has no effect on the kinetic parameters obtained, provided that it is selected in the plateau zone of the TG curve after the drying process.

As indicated above, the selection of the final temperature of the pyrolysis process is more complex since, after the steep reduction of the mass percentage due to the release of the volatile matter of the sample (at around 300 ºC in Figure 7 a)), the mass percentage continues to decrease at a lower rate because of the reduced amount of volatiles and because of the onset of the slow thermal degradation of char (for temperatures above 400 ºC in Figure 7 a)). Unfortunately, the pyrolysis conversion rate does not become zero at high temperatures after the consumption of the volatile matter, due to the continuing slow decomposition of the remaining char. Therefore, the selection of the final temperature of pyrolysis is somewhat arbitrary and may affect the results obtained for the activation energy and the pre-exponential factor of the total mass loss during the pyrolysis process. To quantify this effect, a sensitivity analysis of the value of this final temperature on the values obtained from sDAEM for the kinetic parameters of pyrolysis was carried out. Four values of the final temperature of the pyrolysis process of 450, 600, 750, and 900 ºC were

chosen. The degree of conversion during pyrolysis as a function of temperature for the various final temperatures studied can be seen in Figure 7 b). The evolution of the pyrolysis conversion degree with temperature is quite similar in all cases for values of the degree of conversion below 80 %, i.e., for temperatures below 400 ºC, in what is called the active stage of pyrolysis, where pyrolysis of hemicellulose and cellulose, and partly lignin, occurs. However, for higher values of the degree of conversion, i.e., for temperatures between 400 and 900 ºC, the passive stage of pyrolysis takes place, which is dominated by the pyrolysis of the lignin contained in char [63,64]. Significant differences are observed for the evolution of the conversion at temperatures above 400 ºC, depending on the final temperature selected for the pyrolysis process. The differences occurring for these high temperatures are caused by the increasing importance of devolatilization of lignin contained in char at higher temperatures.

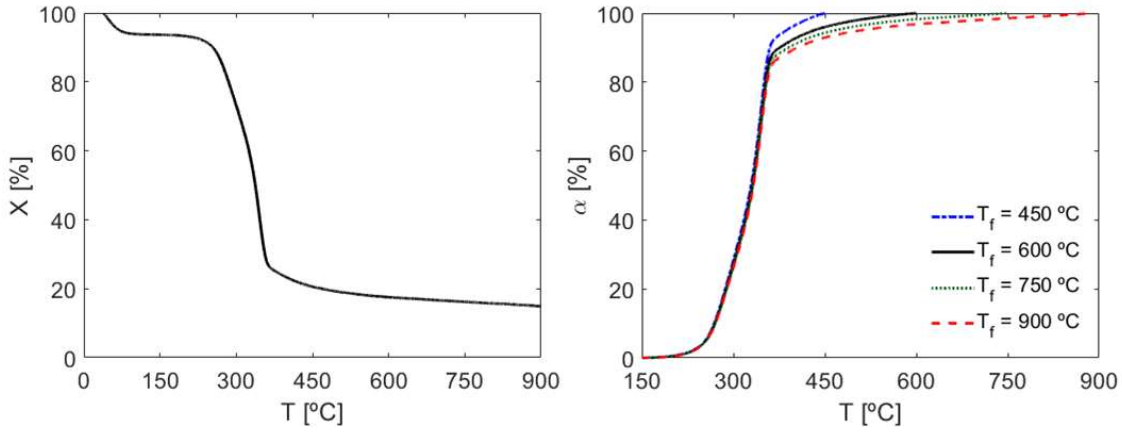

Figure 7: a) Evolution of the percentage of mass remaining with temperature during the pyrolysis of beech wood in the TGA Q500 at 5 ºC/min (pre-dried sample), b) Evolution of the degree of conversion with temperature during the

pyrolysis of beech wood in the TGA Q500 at 5 ºC/min for various final temperatures (pre-dried sample).

Considering the curves of the pyrolysis conversion degree versus temperature depicted in Figure 7 b) for the various final temperatures analyzed, the sDAEM was applied to determine the kinetic parameters of beech wood pyrolysis, i.e., the activation energy and pre-exponential factor, as a function of the degree of conversion for each final temperature selected. The results of the kinetic parameters as a function of the conversion degree are shown in Figure 8. They show similar values for the kinetic parameters derived for α below 80 %. In contrast, for degrees of conversion above 80 %, both the pre-exponential factor and the activation energy increase substantially when the final temperature selected for the pyrolysis process is higher. These differences are caused by the increasing importance of char pyrolysis towards higher final temperatures. For instance, if the final temperature is chosen to be 450 °C, a degree of conversion of 90 % corresponds closely to the end of the release of biomass volatile matter (see Figure 7 a)). However, if the final temperature is chosen to be 900 °C, the same degree of conversion corresponds to the ongoing thermal degradation of the char produced, and of course, these completely different chemical reactions have different kinetic parameters associated. Therefore, the final temperature selected for the pyrolysis process influences the kinetic parameters obtained for high degrees of conversion. It is recommended to select a final temperature up to which the derivative of the mass percentage remaining, *X*, has a low value and starts to decrease steadily. In the present study of beech wood pyrolysis, it was found most appropriate to select a final temperature of 600 °C for the evaluation of the kinetic data.

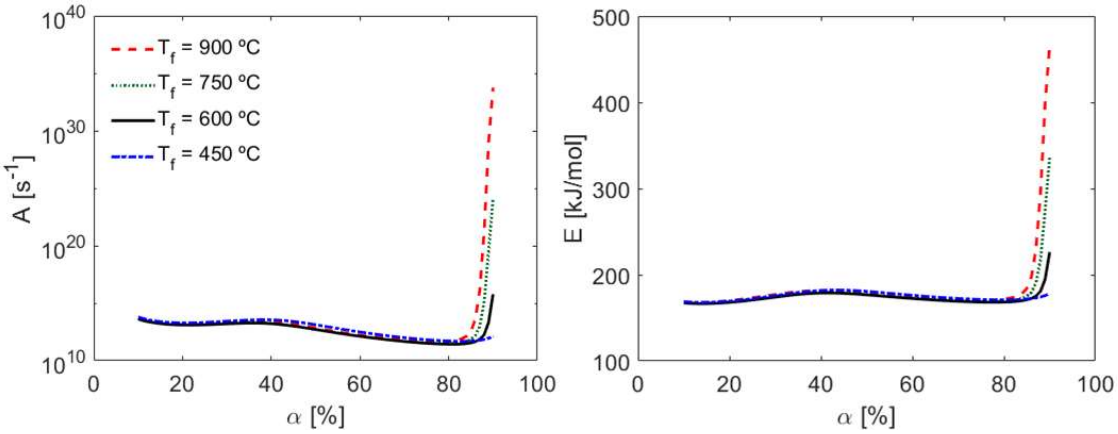

Figure 8: Kinetic parameters obtained from the sDAEM for the pyrolysis measurements of beech wood conducted in the TGA Q500 considering various final temperatures for the pyrolysis process (pre-dried samples).

4.6. Discussion on the capabilities of model-free and model-fitting kinetic methods

As noticed in sections 1 and 2, the values of kinetic parameters derived from TG investigations may show notable differences. These are somewhat difficult to interpret due to the non-linear character of the reaction kinetics. The problem can be solved by choosing a more unifying benchmark for the comparison. In that sense, TG or DTG curves can be reconstructed from the fitted kinetic data which directly illustrate the data quality by comparison to the experimental measurements.

As example, the experiment with a pre-dried sample, pyrolyzed at a heating rate of 25 ºC/min in the TGA Q500, was chosen. The TG curves were recalculated using the kinetic parameters as derived from the sDAEM, integral isoconversional methods of OFW and KAS, Friedman and Kissinger methods, as well as by the five-step model. The recalculated curves of Friedman, OFW, and KAS were obtained by solving their characteristic equations, i.e., Eqs. (4),

(6), and (7), respectively, whereas Eq. (10) was solved to obtain the recalculated curve of sDAEM. In contrast, the recalculated curves of the Kissinger method and the five-step fitting model were derived by integration of dm/dt = - k·m, considering the kinetic parameter to determine the rate coefficient, Eq. (2). The results are shown in Figure 9 and compared to the experimental TG curve. The sDAEM, KAS and OFW methods reproduce the experimental data with high accuracy. The deviations from the measured degree of conversion are less than 0.15 %, hence the three results collapse on a single curve in Figure 9. The other methods give less accurate results in the order Friedman's method > five-step model > Kissinger's method. An extra pyrolysis experiment was conducted at 75 ºC/min, a higher heating rate than those use to derive the kinetic parameters, to check the capability of the kinetic methods to predict TG curves at higher heating rates. The results obtained, also depicted in Figure 9, are similar to those at 25 ºC/min, with a slight shift to higher temperatures of the conversion estimation of the five-step model.

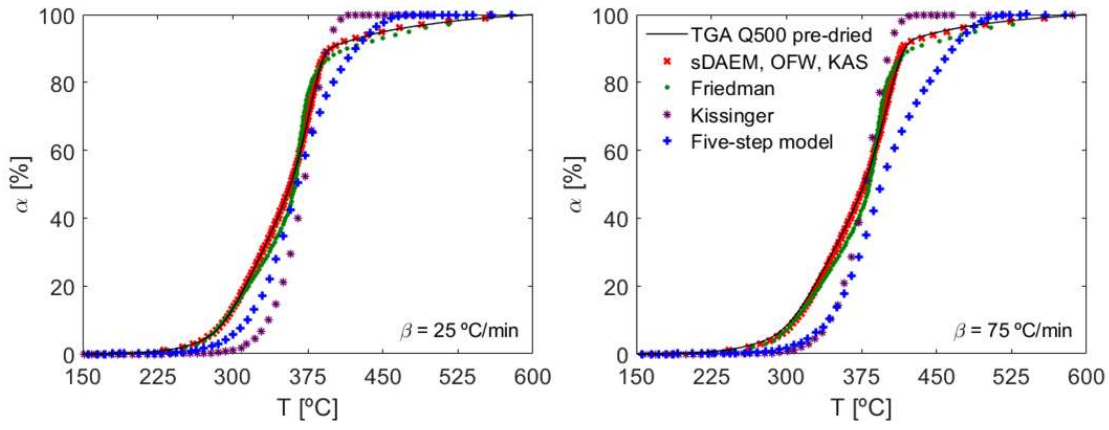

Figure 9: Comparison of the TG curve measured in the TGA Q500 for the pre-dried sample and the recalculated curves obtained by the kinetic models at 25 ºC/min and 75 ºC.

As noticed before, Friedman's model suffers from the differential character of the method and Kissinger's method appears to be an oversimplification in case of mixtures of substances and polymers. Regarding the five-step model, some disagreement with the experimental TG curve was expected according to Figure 6. However, the five-step model also allows an estimate of the pyrolysis gas composition, which is not a subject in this work.

Among the model-free methods, the integral methods OFW, KAS and sDAEM are found to be superior to the differential method of Friedman or the simple Kissinger method. Regarding model-fitting methods, they clearly have the advantage to allow predictions of the pyrolysis gas composition, in contrast, they often appear to have problems to reproduce the final, slow pyrolysis of char correctly. It appears that for wood pyrolysis, there is no direct comparison of several model-fitting methods available in the literature.

5. Conclusions

The kinetics of beech wood pyrolysis was studied by means of non-isothermal thermogravimetric measurements conducted in two different thermogravimetric analyzers (TGA), a TG 209/2/F from Netzsch and a TGA Q500 from TA Instruments. Both instruments were found to have a high repeatability and accuracy for the temperature control. Model-free methods, isoconversional models, the simplified distributed activation energy model (sDAEM), and a model-fitting method, the five-step model, were used to determine the kinetic parameters of the pyrolysis reactions. Except for Kissinger's method, the kinetic parameters, obtained from the experimental results in both analyzers were in very good agreement. The kinetic data obtained from the different evaluation

methods were compared by reconstruction of the thermogravimetric curves. In this way, the performance of methods of Ozawa, Flynn and Wall (OFW), Kissinger-Akahira-Sunose (KAS) and sDAEM were found to be excellent. Friedman's method, Kissinger's method and the five-step model gave somewhat less good results, partly due to the corresponding mathematical procedure and partly due to the adopted simplifications. Hence, from the point of view of accurate data approximation, the integral isoconversional methods and sDAEM are recommended. From the point of view of detailed mechanistic information and product formation, model-fitting methods are required, probably increasing the accuracy with an increasing number of reactions, with sDAEM representing the limiting case of an infinite set of reaction steps.

In addition, the pyrolysis process was analyzed for pre-dried beech wood samples and for in situ dried samples, i.e., for a sample dried in the TGA as an immediate process prior to the pyrolysis. The in situ dried sample was found to pyrolyze faster than the pre-dried sample, and the experimental pyrolysis rates were close to those of the five-step model. The effect of the final temperature selected for the pyrolysis process was also analyzed, finding that both the pre-exponential factor and the activation energy increased significantly for higher values of the final pyrolysis temperature, as a consequence of the greater importance of the slow thermal degradation of char at elevated temperatures.

Acknowledgments

The authors express their gratitude to the BIOLAB experimental facility, to the "Programa de movilidad de investigadores en centros de investigación extranjeros (Modalidad A)" from the Carlos III University of Madrid (Spain) and

to the Institute of Combustion Technology at DLR for the financial support conceded to Antonio Soria-Verdugo for a research stay at the German Aerospace Center DLR (Stuttgart, Germany) during the summer of 2018.

Funding by the Helmholtz Association of German Research Centers in the research fields energy, fuels and gasification, especially in the Program “Energy Efficiency, Materials and Resources“, is acknowledged by the Institute for Technical Chemistry at KIT, Karlsruhe, and by the Institute of Combustion Technology at DLR Stuttgart.

References

[1] Asadullah M. Barriers of commercial power generation using biomass gasification gas: a review. Renew Sustain Energy Rev 2014; 29, 201-215.

[2] McKendry P. Energy production from biomass (part 2): conversion technologies. Bioresour. Technol. 2002; 83, 47-54.

[3] Basu P. Biomass gasification and pyrolysis - Practical design and theory. Elsevier Inc.; 2010.

[4] Dhyani V., Bhaskar T. A comprehensive review on the pyrolysis of lignocellulosic biomass. Renew Energy 2018; 129, 695-716.

[5] Papadikis K., Gu S., Bridgwater A.V., Gerhauser H. Application of CFD to model fast pyrolysis of biomass. Fuel Process. Technol. 2009; 90, 504-512.

[6] Wang S., Dai G., Yang H., Luo Z. Lignocellulosic biomass pyrolysis mechanism: a state-of-the-art review. Prog. Energy Combust. Sci. 2017; 62, 33-86.

[7] Vyazovkin S., Burnham A.K., Criado J.M., Pérez-Maqueda L.A., Popescu C., Sbirrazzuoli N. ICTAC kinetics committee recommendations for performing kinetic computations on thermal analysis data. Thermochim. Acta 2011; 520, 1-19.

[8] Cai J., Wu W., Liu R. An overview of distributed activation energy model and its application in the pyrolysis of lignocellulosic biomass. Renew. Sust. Energ. Rev. 2014; 36, 236-246.

[9] Anca-Couce A. Reaction mechanisms and multi-scale modelling of lignocellulosic biomass pyrolysis. Prog. Energy Combust. Sci. 2016; 53, 41-79.

[10] Soria-Verdugo A., Goos E., García-Hernando N., Riedel U. Analyzing the pyrolysis kinetics of several microalgae species by various differential and integral isoconversional kinetic methods and the Distributed Activation Energy Model. Algal Res. 2018a; 32, 11-29.

[11] Arrhenius S. Über die Reaktionsgeschwindigkeit bei der Inversion von Rohrzucker durch Säuren (On the reaction velocity of the inversion cane sugar by acids). Z. Phys. Chem. 1889; 4, 226-248.

[12] Hemminger W.F., Cammenga H.K. Methoden der thermischen Analyse. Berlin, Germany, Springer, 1989.

[13] Khawam A., Flanagan D.R. Basics and Applications of Solid-State Kinetics: A Pharmaceutical Perspective. J. Pharm. Sci. 2006; 95, 472-498.

[14] Pérez-Maqueda L.A., Sánchez-Jiménez P.E., Criado J.M. Kinetic Analysis of Solid-State Reactions: Precision of the Activation Energy Calculated by Integral Methods. Int. J. Chem. Kinet. 2005; 37, 658–666.

[15] Broido A., Weinstein M. Kinetics of solid-phase cellulose pyrolysis. In: Wiedemann, ed., Proceedings of the 3rd International Conference on Thermal Analysis. 1971, p. 285-296, Basel, Birkhauser Verlag.

[16] Shafizadeh F. Introduction to pyrolysis of biomass. J. Anal. Appl. Pyrol. 1982; 3, 283-305.

[17] Antal M.J.; Várhegyi G. Impact of Systematic Errors on the Determination of Cellulose Pyrolysis Kinetics. Energy Fuels 1997; 11, 1309-1310.

[18] Conesa J.A., Caballero, J.A., Marcilla, A., Font, R. Analysis of different kinetic models in the dynamic pyrolysis of cellulose. Thermochim. Acta 1995; 254, 175-192.

[19] Lin T., Goos E., Riedel U., A sectional approach for biomass: Modelling the pyrolysis of cellulose. Fuel Processing Technology 2013; 115, 246-253.

[20] Grønli M., Antal M.J., Várhegyi G. A round-robin study of cellulose pyrolysis kinetics by thermogravimetry. Ind. Eng. Chem. Res. 1999; 38, 2238-2344.

[21] Maciejewski M. Computational aspects of kinetic analysis. Part B: The ICTAC Kinetics Project - the decomposition kinetics of calcium carbonate revisited, or some tips on survival in the kinetic mine field. Thermochim. Acta 2000; 355, 145-154.

[22] Antal M.J., Várhegyi G., Jakab E. Cellulose pyrolysis kinetics: Revisited. Ind. Eng. Chem Res.1998; 37, 1267-1275.

[23] Anca-Couce A., Berger A., Zobel N. How to determine consistent biomass pyrolysis kinetics in a parallel reaction scheme. Fuel 2014; 123, 230-240.

[24] Kissinger H.E. Variation of peak temperature with heating rate in differential thermal analysis. J. Res. Natl. Bur. Stand. 1956; 57, 217-221.

[25] Kissinger H.E., Reaction kinetics in differential thermal analysis. Anal. Chem. 1957; 29, 1702-1706.

[26] Vyazovkin S. Isoconversional kinetics. In: Handbook of Thermal Analysis and Calorimetry Vol.5: Recent Advances, Techniques and Applications. 2008, Elsevier B.V. M.E. Brown and P.K. Gallagher (Editors), Chapter 13, pages 503-538.

[27] Friedman H. L. Kinetics of thermal degradation of char-forming plastics from thermogravimetry. Application to a phenolic plastic. J. Polym. Sci. C. 1964; 6, 183-195.

[28] Ozawa T. A new method of analyzing thermogravimetric data. Bull. Chem. Soc. Jpn. 1965; 38, 1881-1886.

[29] Flynn J. H., Wall L. A. General treatment of the thermogravimetry of polymers. J. Res. Nat. Bur. Standards. 1966; 70A, 487-523.

[30] Akahira T., Sunose T. Method of determining activation deterioration constant of electrical insulating materials. Res. Rep. Chiba Inst. Technol. 1971; 16, 22-31.

[31] Vyazovkin S. Evaluation of activation energy of thermally stimulated solid-state reactions under arbitrary variation of temperature. J. Comput. Chem. 1997; 18, 393-402.

[32] Doyle C.D. Estimating isothermal life from thermogravimetric data. J. Appl. Polym. Sci. 1962; 6, 639-642.

[33] P. Murray, J. White. Kinetics of the thermal dehydration of clays. IV. Interpretation of the differential thermal analysis of the clay minerals. Trans. Brit. Ceram. Soc. 1955; 54, 204-238.

[34] M.J. Starink. The determination of activation energy from linear heating rate experiments: a comparison of the accuracy of isoconversion methods. Thermochim. Acta 2003; 404, 163-176.

[35] Vand V. A theory of the irreversible electrical resistance changes of metallic films evaporated in vacuum. Proc. Phys. Soc. 1943; 55, 222-246.

[36] Miura K. A new and simple method to estimate f(E) and $k_0(E)$ in the distributed activation energy model from three sets of experimental data. Energ. Fuel 1995; 9, 302-307.

[37] Miura K., Maki T. A simple method for estimating f(E) and $k_0(E)$ in the distributed activation energy model. Energ. Fuel 1998; 12, 864-869.

[38] Coats A.W., Redfern J.P. Kinetic parameters from thermogravimetric data. Nature. 1964; 201, 68-69.

[39] Soria-Verdugo A., Goos E., García-Hernando N. Effect of the number of TGA curves employed on the biomass pyrolysis kinetics results obtained using the Distributed Activation Energy Model. Fuel Process. Technol. 2015; 134, 360-371.

[40] Soria-Verdugo A., Goos E., Morato-Godino A., García-Hernando N., Riedel U. Pyrolysis of biofuels of the future: Sewage sludge and microalgae - Thermogravimetric analysis and modelling of the pyrolysis under different temperature conditions. Energ. Convers. Manage. 2017; 138, 261-272.

[41] Soria-Verdugo A., Goos E., Arrieta-Sanagustín J., García-Hernando N. Modeling of the pyrolysis of biomass under parabolic and exponential temperature increases using the Distributed Activation Energy Model. Energ. Convers. Manage. 2016; 118, 223-230.

[42] Soria-Verdugo A., Rubio-Rubio M., Goos E., Riedel U. Combining the lumped capacitance method and the simplified distributed activation energy model to describe the pyrolysis of thermally small biomass particles. Energ. Convers. Manage. 2018b; 175, 164-172.

[43] Couhert C., Commandre J.M., Salvador S. Is it possible to predict gas yields of any biomass after rapid pyrolysis at high temperature from its composition in cellulose, hemicellulose and lignin? Fuel 2009; 88, 408-417.

[44] Branca C., Albano A., Di Blasi C. Critical evaluation of global mechanisms of wood devolatilization. Thermochim. Acta 2005; 429, 133-141.

[45] Mätzing H., Gehrmann H.J., Merz D., Kolb T., Seifert H. A five step pyrolysis mechanism for wood burning models. Proceedings of the 19th European Biomass Conference. Berlin, Germany. Florence, Italy: ETA-Florence Renewable Energies, 2011. http://www.etaflorence.it/proceedings/register.asp

[46] Schinkel A.P. Zur Modellierung der Biomassepyrolyse im Drehrohrreaktor,. Ph.D. Thesis, Universität Kassel, Germany, 2002.

[47] Di Blasi C. Modeling chemical and physical processes of wood and biomass pyrolysis. Prog. Energy Comb. Sci. 2008; 34, 47–90.

[48] Ranzi E., Cuoci A., Faravelli T., Frassoldati A., Migliavacca G., Pierucci S., Sommariva S. Chemical kinetics of biomass pyrolysis. Energy Fuels 2008; 22, 4292–4300.

[49] Tomasi Morgano M., Leibold H., Richter F., Seifert H. Screw pyrolysis with integrated sequential hot gas filtration. J. Anal. Appl. Pyrol. 2015; 113, 216-224.

[50] Mätzing H., Gehrmann H.J., Seifert H., Stapf D. Modelling grate combustion of biomass and low rank fuels with CFD application. Waste Manage 2018; 78, 686-697.

[51] Mätzing H., Baris D., Ciuta S., LeBlanc J., Castaldi M.J., Gehrmann H.J., Stapf D. A comparison of wood pyrolysis products obtained by thermogravimetry and intra-particle measurements. 6th International Conference on Engineering for Waste and Biomass Valorisation (WasteEng 2016), Albi, France, 2016 p. 510-517.

[52] Tomasi Morgano M. Screw pyrolysis of biogenic feedstock with integrated hot gas filtration. PhD thesis, University of Stuttgart, 2019.

[53] Beuth; 2019. https://www.beuth.de/de/regelwerke, https://europa.eu/european-union/business/eu-standards_de

[54] Klemm D., Philipp B., Heinze T., Heinze U., Wagenknecht W. Comprehensive Cellulose Chemistry: Fundamentals and Analytical Methods, Volume 1. Wiley, 1998.

[55] Vyazovkin S., Chrissafis K., di Lorenzo M.L., Koga N., Pijolat M., Roduit B., Sbirrazzuoli N., Suñol J.J. ICTAC Kinetics Committee recommendations for collecting experimental thermal analysis data for kinetic computations. Thermochim. Acta, 2014; 590, 1-23.

[56] Soria-Verdugo A., García-Hernando N., Garcia-Gutierrez L.M., Ruiz-Rivas U. Analysis of biomass and sewage sludge devolatilization using the distributed activation energy model. Energ. Convers. Manage. 2013; 65, 239-244.

[57] Soria-Verdugo A., Garcia-Gutierrez L.M., Blanco-Cano L., Garcia-Hernando N., Ruiz-Rivas U. Evaluating the accuracy of the Distributed Activation Energy Model for biomass devolatilization curves obtained at high heating rates. Energ. Convers. Manage. 2014; 86, 1045-1049.

[58] Lei Q., Xie Q., Ding Y. Fire hazard evaluation of activated carbons. J. Therm. Anal. Calorim. 2020; 139, 441-449.

[59] Radhakrishnan K., Hindmarsh, A. Description and use of LSODE, the Livermore solver for ordinary differential equations, Technical report UCRL-ID-113855, Lawrence Livermore National Laboratory, 1993.

[60] Munir S., Daood S.S., Nimmo W., Cunliffe A.M., Gibbs B.M. Thermal analysis and devolatilization kinetics of cotton stalk, sugar cane bagasse and shea meal under nitrogen and air atmospheres. Bioresour. Technol. 2009; 100, 1413-1418.

[61] Tonbul Y., Saydut A., Yurdakoc K., Hamamci C. A kinetic investigation on the pyrolysis of Seguruk asphaltite. J. Therm. Anal. Calorim. 2009; 95, 197-202.

[62] Ding Y., Ezekoye O.A., Lu S., Wang C. Thermal degradation of beech wood with thermogravimetry/Fourier transform infrared analysis. Energ. Convers. Manage. 2016; 120, 370-377.

[63] Grønli M.G., Várhegyi G., Di Blasi C. Thermogravimetric analysis and devolatilization kinetics of wood. Ind. Eng. Chem. Res. 2002; 41, 4201-4208.

[64] Di Blasi C., Branca C. Kinetics of primary formation from wood pyrolysis. Ind. Eng. Chem. Res. 2001; 40, 5547-5556.

[65] K.G. Mansaray, A.E. Ghaly. Thermal degradation of rice husks in nitrogen atmosphere. Bioresour. Technol. 1998; 65, 13-20.

[66] K. Slopiecka, P. Bartocci, F. Fantozzi. Thermogravimetric analysis and kinetic study of poplar wood pyrolysis. Appl. Energ. 2012; 97, 491-497.

List of figures

Figure 9: Comparison of the TG curve measured in the TGA Q500 for the pre-dried sample and the recalculated curves obtained by the kinetic models at 25 ºC/min and 75 ºC.

List of tables